Chemical Science

ROYAL SOCIETY OF CHEMISTRY

EDGE ARTICLE

View Article Online
View Journal | View Issue

Cite this: *Chem. Sci.*, 2022, **13**, 9713

All publication charges for this article have been paid for by the Royal Society of Chemistry

Received 23rd June 2022
Accepted 30th July 2022

DOI: 10.1039/d2sc03518a

rsc.li/chemical-science

Visible light activated BINOL-derived chiroptical switches based on boron integrated hydrazone complexes†

Sven van Vliet,[a] Georgios Alachouzos,[a] Folkert de Vries,[a] Lukas Pfeifer[b] and Ben L. Feringa*[a]

Chiral optical switches, which use light to control chirality in a reversible manner, offer unique properties and fascinating prospects in the areas of molecular switching and responsive systems, new photochromic materials and molecular data processing and storage. Herein, we report visible light responsive chiroptical switches based on tetrahedral boron coordination towards an easily accessible hydrazone ligand and optically pure BINOL. Upon instalment of a non-planar dibenzo[*a*,*d*]-cycloheptene moiety in the hydrazone ligand's lower half, the enantiopure boron complex shows major chiroptical changes in the CD read-out after visible light irradiation. The thermal isomerization barrier in these chiroptical switching systems showed to be easily adjustable by the introduction of substituents onto the olefinic bond of the cycloheptene ring, giving profound control over their thermal stability. The control over their thermal stability in combination with excellent reversibility, photochemical properties and overall robustness of the complexes makes these BINOL-derived chiroptical switches attractive candidates for usage in advanced applications, *e.g.* photonic materials and nanotechnology.

Introduction

Molecular photochromic switches, where two states are photochemically interconverted, hold great promise in, amongst others, the fields of molecular memory and data storage, supramolecular chemistry and nanotechnology.[1–11] The exploitation of light as a stimulus offers the exceptional possibility of gaining high spatial temporal control whilst remaining non-invasive and waste-free. Over the past decades, a wide variety of photochromic switches, such as azobenzenes,[12–14] (stiff)stilbenes,[15,16] overcrowded alkenes,[17–19] diarylethenes,[20,21] spiropyrans[22,23] and (acyl) hydrazone switches,[24–26] all possessing a unique set of photophysical properties, have been investigated. Recently, there has been a major interest in the development of switches addressable upon visible light irradiation in order to move away from the highly energetic and potentially damaging ultraviolet (UV) excitation wavelengths.[27–32] Illustrative are the tetra-ortho substituted azobenzenes designed by Woolley *et al.*[33] and the easily accessible azo-BF_2 complexes designed by Aprahamian and co-workers where the photoisomerization of the hydrazone-based ligand is solely performed using visible[34] or near infrared light.[35]

For the majority of the photochromic switches, sampling in the absorption bands using UV-vis spectroscopy is the most common method for detection of isomerization. However, this readout process concomitantly induces excitation and subsequent interconversion between the two states, which might lead towards destruction of photochromic memory after several readout operations.[1,2,36] In that respect, chiral optical switches are a privileged class of photochromic molecules, as nondestructive readout of such systems is feasible by monitoring the optical rotation at wavelengths remote from the excitation wavelengths.[37,38] Various chiral switching systems based on photochromic molecules have been developed: (a) stereospecific photochemical interconversion of enantiomers using circularly polarized light (CPL),[39] (b) the photoisomerization of two bistable diastereomeric forms, *i.e.* P and M′ helices, using two different excitation wavelengths[37,40–42] and (c) the instalment of an achiral photochromic unit (A) onto a chiral auxiliary.[21,38] A major advantage of the latter approach is the possibility of using an enantiopure chiral auxiliary, hereby circumventing the need for tedious HPLC separation of enantiomers or diastereomers after preparation as is the case in methods a and b.

The 1,1′-bi-2-naphthol (BINOL) scaffold has received considerable interest as chiral auxiliary in chiroptical switching systems[43] and chiral dopant in liquid crystalline material[44] as both enantiomers can be readily separated and are highly stable

[a]*Stratingh Institute for Chemistry, Zernike Institute for Advanced Materials, University of Groningen, Nijenborgh 4, Groningen 9747 AG, Netherlands. E-mail: B.L.Feringa@rug.nl*

[b]*EPFL, CH G1 614 (Bâtiment CH), Station 6, Lausanne, CH-1015, Switzerland*

† Electronic supplementary information (ESI) available. CCDC 2181178 and 2181177. For ESI and crystallographic data in CIF or other electronic format see https://doi.org/10.1039/d2sc03518a

towards racemization. The intrinsic axial chirality of the BINOL framework was used for photoinduced chiroptical switching of the handedness of cholesteric phases in a liquid crystal matrix upon instalment of two photochromic azobenzene moieties (A) at the 5,5′ positions remote from its C2-axis.[45] In a related system, the photoisomerizable azobenzene modalities were inserted on the 2,2′- positions of the optically pure binapthyl core, thereby altering the dihedral angle between the two naphthalene regions upon irradiation.[46] Although these chiroptical switches allow for a change in circular dichroism (CD) readout upon irradiation, their overall applicability is limited due to non-orthogonal switching behavior of both azobenzene moieties, modest change in molar ellipticity upon irradiation, the usage of UV excitation in one of the isomerization directions, long irradiation times and multiple synthesis and purification steps.

Taking inspiration from the visible light responsive azo-BF_2 complexes discovered by Aprahamian and co-workers,[34,35] in combination with our longstanding expertise in the exploitation of BINOL as versatile ligand in asymmetric catalysis,[47] we devised BINOL-derived chiroptical switches based on boron integrated hydrazone complexes. As boron shows high affinity for nitrogen containing ligands as well towards bidentate diols, it was envisioned that co-complexation of optically active BINOL and an easily accessible, hydrazone ligand possessing two nitrogen coordination sites, *i.e.* a bidentate ligand, onto a boron centre would yield a potential chiroptical switch. We envision a system based on condensation of pyridyl hydrazine onto a rigid, tricyclic diaryl ketone affording a privileged hydrazone-based ligand, as coordination of the hydrazino nitrogen lone pair at the boron centre brings the switching axis, the C=N bond, in close proximity to the BINOL framework. In other words, we expect the rigid lower half of the hydrazone ligand to sterically interact with this chiral auxiliary to induce a helical geometry within the structure, leading to an inversion of the overall helicity of the complex upon irradiation resulting in a substantial change in molar circular dichroism and thereby generating robust CD readout.

Results and discussion

Starting from condensation reactions involving commercially available 2-hydrazinopyridine and rigid, diaryl ketones, such as fluorenone (**X** = –) and dibenzosuberenone (**X** = C_2H_2), the bidentate hydrazone ligands were obtained in good yields (Fig. 1). The tendency of boron to form tetracoordinated dimeric complexes in the presence of bidentate diols, such as (*R*)-BINOL,[48] prompted us to apply a demethylative direct borylation methodology. The key step is the boron-mediated demethylation of the doubly methylated phenolic BINOL moiety followed by consecutive addition of the hydrazone facilitated by a Brønsted base resulting in the formation of strongly coloured, optically pure complexes **1** to **4**. An asymmetric fluorene-based hydrazone was used in complexes **1** and **2** in order to probe the viability of photoisomerization of such tetracoordinated boron complexes based on the change in *cis–trans* ratio during irradiation. Complexes **3** and **4** were designed

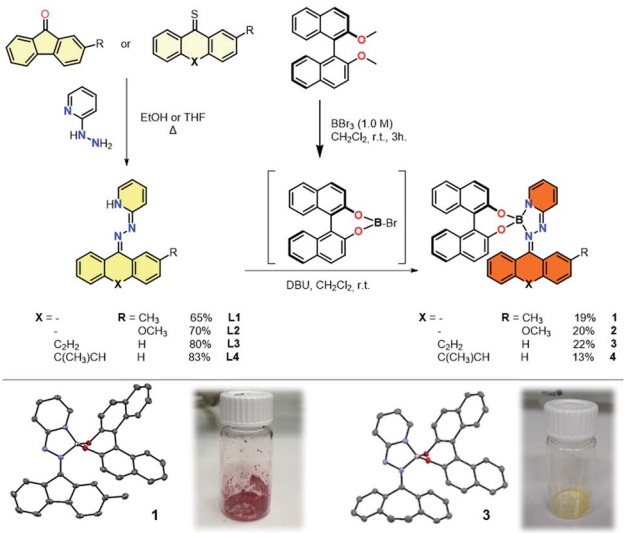

Fig. 1 Top: synthesis of chiral tetracoordinated boron-integrated hydrazone complexes *via* demethylative direct borylation. Bottom: crystal structures of complexes **1** and **3**. Structures are showing 50% probability ellipsoids; hydrogens and solvents are omitted for clarity.

to further distort the planarity of the hydrazone ligand, leading to an overall helical geometry of these complexes. Steric obstruction within these complexes is expected upon switching and thereby imposing potential thermodynamically unfavourable, metastable isomers with inverted helicities.

Single crystals of complexes **1** and **3** suitable for X-ray diffraction were grown by slow diffusion of hexane into methylene chloride (CH_2Cl_2) at 5 °C (Fig. 1 and S6†). In both cases, tetrahedral geometry around the boron centre was observed. The boron coordination with the pyridyl nitrogen along with the hydrazino nitrogen forms a five-membered ring, bringing the optically pure BINOL ligand in close proximity to the switching unit of complex **1**, having N–B bond lengths of 1.566(4) and 1.634(4) Å, respectively. The instalment of a rigid, non-planar cycloheptene-based hydrazone in complex **3** had no significant influence on the N–B bond lengths as those are respectively 1.556(2) and 1.629(2) Å. As both bidentate ligand are connected in tetrahedral fashion around the central boron atom, complexes **1** and **3** are classified as heterocyclic spiro compounds experiencing axial chirality (S_a). In the solid state, these complexes are bench stable under aerobic conditions for a period over two years.

In order to examine the photophysical behaviour of complex **2** in solution, the photoisomerization was studied by UV-vis and ^{1}H NMR spectroscopy (Fig. 2 and S5†). Prolonged irradiation using cyan light (528 nm) of a thermally equilibrated *trans*-enriched NMR sample (CD_2Cl_2, 293 K) led to change in *trans–cis* ratio until the photostationary state (PSS 48 : 52) was reached. As both isomers display identical UV-vis spectra, reversed photoinduced isomerization to the initial state is not feasible. We found additional evidence of *cis–trans* isomerization when we compared LCMS spectra of compound **2** before and after irradiation. These results show such complexes can be photochemically isomerized using visible light, yet the rigid fluorene-

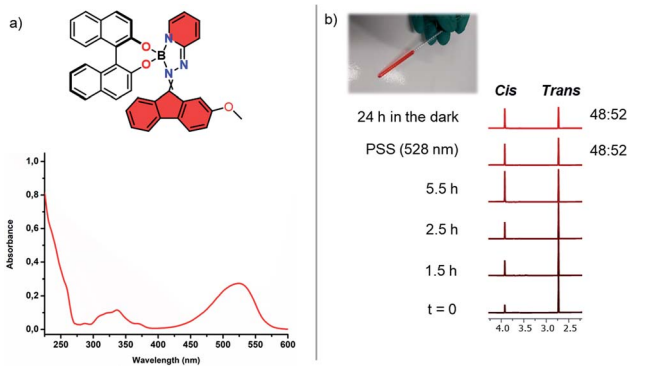

Fig. 2 (a) UV-vis spectrum of complex **2** (CH_3CN, 298 K, 10^{-5} M) (b) Photoisomerization of **2** using 528 light nm probed by the intensities of the methoxy resonances over time (CD_2Cl_2, 298 K, 400 MHz).

based part of the hydrazone ligand does not induce helicity in complex **2** meaning there is negligible steric congestion with the BINOL framework upon switching. As a consequence of the absence of steric obstruction, there is no thermal isomerization towards the initial state at ambient temperatures. Nevertheless, it has been shown that steric hindrance in overcrowded alkene based chiroptical switches is fully adjustable and could be tuned by modification of the bridging unit X in the rigid, tricyclic lower half resemblant to the lower half of complex **2**.[49] It can therefore be foreseen that the introduction of a bridging unit in the lower half of such tetracoordinated boron-integrated hydrazone complexes will distort the planarity of the hydrazone ligand, concomitantly altering the isomerization behaviour of the complex. Addition of hydrazine precursor **L3** containing a 5*H*-dibenzo[*a*,*d*]-cycloheptene to the BINOL boron-bromide species gave rise to complex **3** containing an olefin bridge (**X** = $-C_2H_2-$), which was expected to increase the steric interaction between the non-planar 5*H*-dibenzo[*a*,*d*]-cycloheptene moiety and BINOL's dihedral angle upon irradiation resulting in a higher energetic species. With compound **3** in hand we observed that it also exhibits a hypsochromic absorption shift in comparison to complex **2**, as the non-planarity of the diaryl cycloheptatriene ring partially disrupts the conjugation throughout the hydrazone ligand leading to a broad absorption band located at 455 nm (S3). The CD spectrum of **3** shows multiple cotton effects, starting ($\lambda_{max} \sim 440$ nm, $\lambda_{max} \sim 340$ nm and $\lambda_{max} \sim 230$ nm) with a negative-to-positive induced CD couplet ($\lambda_{max} \sim 440$ nm).[50] Irradiation of a solution of complex **3** (CH_3CN, 10^{-5} M) using 455 nm led to a drastic change in its circular dichroism over a range from 220 to 500 nm. This change in the CD spectrum is indicative for the formation of the metastable species **3′** (Fig. 3 and S4†), resulting from the change in helicity between the 5*H*-dibenzo[*a*,*d*]-cycloheptene and the BINOL-boron moieties. After 10 min of irradiation, no further changes were observed in the CD spectrum, meaning PSS was reached. Storing the irradiated sample in the dark at ambient temperature led to recovery of the initial spectrum within 90 min ($t_{1/2} = 12$ min, S4). The isosbestic points ($\lambda = 365$, 325, 290 and 260 nm) in the CD spectra demonstrate that only two species are involved in the isomerization process. Repeated cycles of irradiation and thermal equilibration confirm the excellent reversibility of this process as no fatigue was observed. The photoinduced formation of the metastable state was further proven by ^{1}H NMR spectroscopy (Fig. 3b and S5†). Irradiation at 455 nm of a thermally equilibrated NMR sample of complex **3** at 0 °C gave rise to a new set of signals belonging to the metastable species. The measurement took place at 0 °C since this yielded a higher PSS ratio after irradiation. After 90 min, the ratio between thermodynamically stable **3** and its metastable form **3′** did not change any further as determined by signal intensity, resulting in 80% of the metastable state at PSS. Allowance of the irradiated NMR sample to reach 25 °C, to permit the reversed thermal isomerization to occur, gave full recovery of the original spectrum recorded at 0 °C. It is known that thermal isomerization barriers of diaryl cycloheptatriene based systems are tuneable and can be altered by the introduction of substituents onto the double bond.[51,52] To illustrate the tunability of the thermally activated C=N isomerization, responsible for the reverse isomerization process from the metastable state back to the stable state, a methyl substituent was installed onto the olefinic double bond of the dibenzo[*a*,*d*]-cycloheptene based hydrazone in order to obtain complex **4** (as a 1 : 1 *E*/*Z* mixture of double bond isomers). As boron complex **4** shows an absorption maximum at 455 nm, its photophysical and thermal behaviour were studied in solution using CD spectroscopy upon irradiation at this particular wavelength (S3). Resembling **3**, a significant change in circular dichroism was observed after 10 min of irradiation, indicative for the formation of the metastable species **4′** (Fig. 4 and S4†). Like compound **3′**, the metastable species **4′**, resulting from the irradiation of **4**, is the result of a change in helicity between the dibenzo[*a*,*d*]-cycloheptene and the BINOL moieties. However, unlike **3**, the original spectrum was not restored by leaving the sample in the dark at 25 °C, which was the first clear indicating the thermal back-relaxation barrier from **4′** to **4** had been increased, therefore slowing down back-relaxation. In fact, the sample had to be heated at 45 °C for several hours ($t_{1/2} = 3.1$ h, S5) in order to reach its thermodynamically stable initial state. The isosbestic points ($\lambda = 360$, 335, 310 and 260 nm) indicate a clean unimolecular conversion. Those findings prove that the barriers for the thermally activated reversed isomerization and thereby the thermal stability of these kind of chiroptical switches are fully adjustable, opening pathways for their usage in soft supramolecular materials, molecular memory and data storage.

Density Functional Theory (DFT) was used to gain more insight into the difference in back-relaxation rates from metastable to stable between **3** and it's methylated homolog **4**. We optimized S_0 ground state and both the S_1 excited state and the T_1 excited state (accessed after intersystem crossing) of both stable and metastable states of **3** or **4**, in addition to transition states leading between each stable and metastable state at the MN15/Def2SVP/SMD = MeCN level (see ESI† for full computational details).[53–55] From our calculations we found that both **3** and **4** exhibit very low interconversion barriers for the excited state stable to metastable isomerization in either the singlet S_1 or the triplet T_1 excited states (**3**: S_1 $\Delta G^{\ddagger}_{inv} = 5.2$ kcal mol^{-1}, T_1

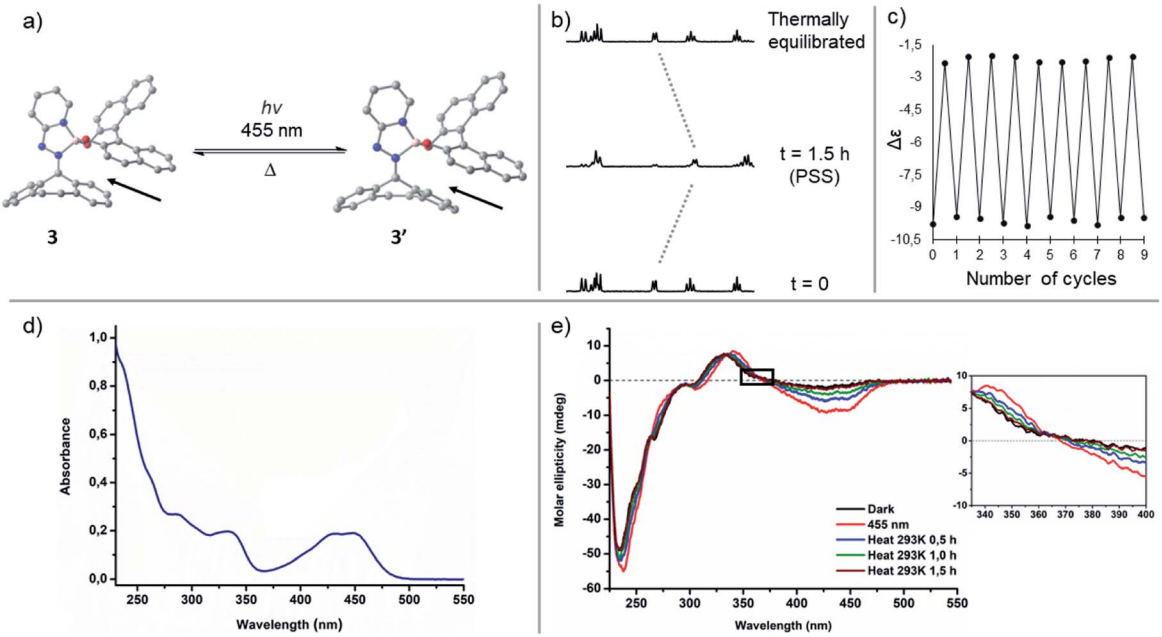

Fig. 3 (a) Geometries obtained after optimization at the MN15/Def2SVP/SMD = MeCN level of stable complex **3** and its metastable species **3′**, formed upon photoisomerization. The markers indicate the helicity change upon irradiation. (b) ^{1}H NMR spectra of **3** before irradiation, irradiated (455 nm) and after thermal equilibration (CD_2Cl_2, 500 MHz) (c) Cycles of thermal equilibration (90 min) and irradiation (455 nm) while monitoring molar ellipticity at 430 nm (d) UV-vis spectrum of **3** (CH_3CN, 298 K) (e) CD spectra of **3** before irradiation, irradiated (455 nm) and after thermal equilibration (CH_3CN, 298 K).

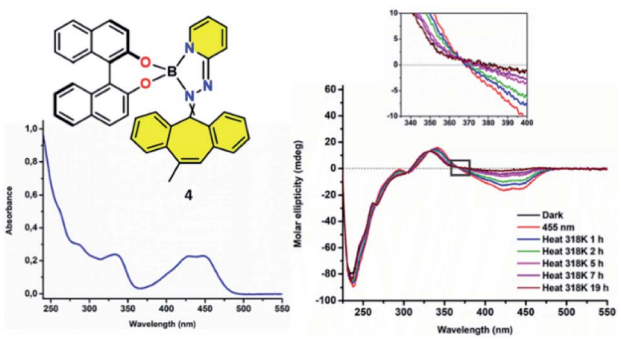

Fig. 4 UV-vis spectrum and CD spectra of **4** before irradiation, during irradiation (455 nm) and after heating (CH_3CN, 10^{-5} M).

$\Delta G^{\ddagger}_{inv}$ = 5.5 kcal mol^{-1}; **4**, averaged for both *E*/*Z* isomers: S_1 $\Delta G^{\ddagger}_{inv}$ = 5.3 kcal mol^{-1}, T_1 $\Delta G^{\ddagger}_{inv}$ = 5.5 kcal mol^{-1}). The low barrier for this excited state inversion is attributed to the lengthening of the C–N hydrazone double bond in the excited state calculated geometries, which adopts considerable single-bond character in the excited state S_1 or T_1. Our calculations also showed that a sufficient thermodynamic driving force was present for the light-triggered stable **3**/**4** to metastable **3′**/**4′** inversion (**3**: S_1 $\Delta G^{\ddagger}_{inv}$ = −10.2 kcal mol^{-1}, T_1 $\Delta G^{\ddagger}_{inv}$ = −10.7 kcal mol^{-1}; **4**, averaged for both *E*/*Z* isomers: S_1 $\Delta G^{\ddagger}_{inv}$ = −6.3 kcal mol^{-1}, T_1 $\Delta G^{\ddagger}_{inv}$ = −9.6 kcal mol^{-1}). These findings suggest that the inclusion of a methyl group into the olefin moiety in **4** had little influence on the excited state stable and metastable state interconversion properties of these systems.

However, one key difference identified between **3** and homolog **4** from our DFT thermochemistry calculations involved the ground state metastable **3′**/**4′** to stable **3**/**4** back-relaxation barriers. In the case of **3′** to **3**, a modest barrier for the back-relaxation (S_0 $\Delta G^{\ddagger}_{inv}$ = 25.1 kcal mol^{-1}) was found. On the contrary, in the case of **4′** to **4**, a slightly higher barrier for the back-relaxation (S_0 $\Delta G^{\ddagger}_{inv}$ = 27.1 or 28.2 kcal mol^{-1}, depending on the configuration of the double bond isomer) was found, suggesting the inclusion of a methyl group into the olefin moiety had destabilizing influence on the ground state inversion transition state, likely the result of 1,4-allylic strain between the methyl group and the proximal aromatic C–H bonds. These DFT analyses are in qualitative agreement with the experimental findings where **4** exhibits a much slower back-relaxation from metastable state back to stable state, when compared to **3**. Overall, these computational insights confirm that a simple introduction of steric bulk into these systems (*i.e.* in the case of **4**, simple methylation of the olefin moiety in **3**) allows for excellent tunability of the metastable state (**3′** or **4′**) lifetime, all while leaving the efficiency of the photochemical switching from stable to metastable state intact.

Conclusions

In conclusion, we have shown a new class of chiroptical switches based on co-complexation in a tetrahedral fashion around a boron centre of an optically pure BINOL auxiliary and readily accessible hydrazone ligands. Upon incorporation of a dibenzo[*a*,*d*]-cycloheptene moiety in the lower half of the photoresponsive hydrazone ligand, visible light irradiation of

the complex leads to the formation of a metastable species accompanied by a major change in circular dichroism giving a powerful CD readout. The visible light-activated chiroptical switch exhibits good PSS (80 : 20) and excellent reversibility over the course of several switching cycles. The fact the reversed thermal isomerization barrier in these chiroptical switches can be easily altered by the introduction of substituents onto the olefinic double bond of the cycloheptene ring gives extensive control over their thermal stability, paving the way for a wide variety of applications.

Data availability

Crystallographic data for compound **1** and **3** has been deposited at the CCDC under deposition numbers 2181178 (complex **1**) and 2181177 (complex **3**) and are available free of charge.

Author contributions

B. L. F. designed the study. S. V. V. synthesized the investigated compounds and performed NMR, CD and UV-vis experiments. G. A. performed DFT calculations. F. D. V. and L. P. performed the X-ray experiments and analysed the data. B. L. F. supervised the work. S. V. V. and G. A. wrote the paper. All authors discussed and commented on the manuscript. B. L. F. acquired funding.

Conflicts of interest

The authors declare there to be no conflicts of interest.

Acknowledgements

S. V. V. gratefully acknowledges A.S. Lubbe for fruitful discussions and revising the manuscript. J. L. Sneep is acknowledged for performing HRMS experiments. J. Y. De Boer is gratefully acknowledged for assistance on synthesis and purification. J. G. H. Hermens is thanked for assistance on the figures. We are grateful for the generous financial support to B. L. F. (the Ministry of Education, Culture and Science of the Netherlands Gravitation Programme No. 024.001.035), to G. A. (EMBO LTF-232-2020 Postdoctoral Fellowship) and to L. P. (Marie Skłodowska-Curie Actions Individual Fellowship No. 793082) We thank the Centre for Information Technology of the University of Groningen for their support and for providing access to the Peregrine high performance computing cluster.

Notes and references

1 B. L. Feringa and W. R. Browne, in *Molecular Switches*, Wiley-VCH, Weinheim, 2011.
2 J. D. Harris and I. Aprahamian, *Proc. Natl. Acad. Sci. U. S. A.*, 2018, **115**, 9414–9422.
3 A. G. Hanssens, F. Eisenreich and S. Hecht, *Adv. Mater.*, 2020, **32**, 1905966.
4 M. Irie, T. Fukaminato, K. Matsuda and S. Kobatake, *Chem. Rev.*, 2014, **114**, 12174–12277.
5 V. Balzani, A. Credi, and M. Venturi, in *Molecular Devices and Machines*, Wiley-VCH, Weinheim, 2008.
6 W. R. Browne and B. L. Feringa, *Nat. Nanotechnol.*, 2006, **1**, 25–35.
7 M. Baroncini, S. Silvi and A. Credi, *Chem. Rev.*, 2020, **120**, 200–268.
8 A. S. Lubbe, T. Van Leeuwen, S. J. Wezenberg and B. L. Feringa, *Tetrahedron*, 2017, **73**, 4837–4848.
9 B. L. Feringa, *Angew. Chem., Int. Ed.*, 2017, **56**, 11060–11078.
10 S. Krause and B. L. Feringa, *Nat. Rev. Chem.*, 2020, **4**, 550–562.
11 R. Costil, M. Holzheimer, S. Crespi, N. A. Simeth and B. L. Feringa, *Chem. Rev.*, 2021, **121**, 13213–13237.
12 H. M. Dhammika Bandara and S. C. Burdette, *Chem. Soc. Rev.*, 2012, **41**, 1809–1825.
13 J. Volarić, W. Szymanski, N. A. Simeth and B. L. Feringa, *Chem. Soc. Rev.*, 2021, **50**, 12377–12449.
14 M. Dong, A. Babalhavaeji, S. Samanta, A. A. Beharry and G. A. Woolley, *Acc. Chem. Res.*, 2015, **48**, 2662–2670.
15 D. Villarón and S. J. Wezenberg, *Angew. Chem., Int. Ed.*, 2020, **59**, 13192–13202.
16 S. J. Wezenberg, L. J. Chen, J. E. Bos, B. L. Feringa, E. N. W. Howe, X. Wu, M. A. Siegler and P. A. Gale, *J. Am. Chem. Soc.*, 2022, **144**, 331–338.
17 B. De Lange, W. F. Jager and B. L. Feringa, *J. Chem. Soc., Chem. Commun.*, 1993, **3**, 288–290.
18 H. A. Van Doren, N. P. M. Huck and B. L. Feringa, *J. Am. Chem. Soc.*, 1995, **117**, 9929–9930.
19 N. P. M. Huck and B. L. Feringa, *J. Chem. Soc., Chem. Commun.*, 1995, **11**, 1095–1096.
20 M. Irie, T. Fukaminato, K. Matsuda and S. Kobatake, *Chem. Rev.*, 2014, **114**, 12174–12277.
21 Z. Zheng, H. Hu, Z. Zhang, B. Liu, M. Li, D. H. Qu, H. Tian, W. H. Zhu and B. L. Feringa, *Nat. Photonics*, 2022, **16**, 226–234.
22 L. Kortekaas and W. R. Browne, *Chem. Soc. Rev.*, 2019, **48**, 3406–3424.
23 R. Klajn, *Chem. Soc. Rev.*, 2014, **43**, 148–184.
24 D. J. Van Dijken, P. Kovaříček, S. P. Ihrig and S. Hecht, *J. Am. Chem. Soc.*, 2015, **137**, 14982–14991.
25 I. Aprahamian, *Chem. Commun.*, 2017, **53**, 6674–6684.
26 M. N. Chaur, D. Collado and J. M. Lehn, *Chem. – Eur. J.*, 2011, **17**, 248–258.
27 D. Bléger and S. Hecht, *Angew. Chem., Int. Ed.*, 2015, **54**, 11338–11349.
28 L. N. Lameijer, S. Budzak, N. A. Simeth, M. J. Hansen, B. L. Feringa, D. Jacquemin and W. Szymański, *Angew. Chem., Int. Ed.*, 2020, **59**, 2–10.
29 C. Petermayer, S. Thumser, F. Kink, P. Mayer and H. Dube, *J. Am. Chem. Soc.*, 2017, **139**, 15060–15067.
30 C. Petermayer and H. Dube, *J. Am. Chem. Soc.*, 2018, **140**, 13558–13561.
31 M. M. Lerch, W. Szymański and B. L. Feringa, *Chem. Soc. Rev.*, 2018, **47**, 1910–1937.
32 M. M. Lerch, M. J. Hansen, W. A. Velema, W. Szymański and B. L. Feringa, *Nat. Commun.*, 2016, **7**, 12054.

33 A. A. Beharry, O. Sadovski and G. A. Woolley, *J. Am. Chem. Soc.*, 2011, **133**(49), 19684–19687.
34 Y. Yang, R. P. Hughes and I. Aprahamian, *J. Am. Chem. Soc.*, 2012, **134**, 15221–15224.
35 Y. Yang, R. P. Hughes and I. Aprahamian, *J. Am. Chem. Soc.*, 2014, **136**, 13190–13193.
36 W. F. Jager, B. De Lange and B. L. Feringa, *Tetrahedron*, 1993, **49**, 8267–8310.
37 A. M. Schoevaars, N. P. M. Huck and B. L. Feringa, *Adv. Mater.*, 1996, **8**, 681–684.
38 E. M. Geertsema, N. Koumura, R. A. Van Delden and B. L. Feringa, *Chem. Rev.*, 2000, **100**, 1789–1816.
39 N. P. M. Huck, W. F. Jager, B. De Lange and B. L. Feringa, *Science*, 1996, **273**, 1686–1688.
40 E. G. Meijer, B. De Lange, W. F. Jager and B. L. Feringa, *J. Am. Chem. Soc.*, 1991, **113**, 5468–5470.
41 R. A. Van Delden, M. B. Van Gelder, N. P. M. Huck and B. L. Feringa, *Adv. Funct. Mater.*, 2003, **13**, 319–324.
42 R. A. Van Delden, M. K. J. Ter Wiel and B. L. Feringa, *Chem. Commun.*, 2004, **2**, 200–201.
43 H. Wang, H. K. Bisoyi, A. M. Urbas, T. J. Bunning and Q. Li, *J. Am. Chem. Soc.*, 2019, **141**, 8078–8082.
44 R. Eelkema and B. L. Feringa, *Org. Biomol. Chem.*, 2006, **4**, 3729–3745.
45 R. A. Van Delden, T. Mecca, C. Rosini and B. L. Feringa, *Chem. – Eur. J.*, 2004, **10**, 61–70.
46 S. Pieraccini, S. Masiero, G. P. Spada and G. Gottarelli, *Chem. Commun.*, 2003, **5**, 598–599.
47 J. F. Teichert and B. L. Feringa, *Angew. Chem., Int. Ed.*, 2010, **49**, 2486–2528.
48 C. Carter, S. Fletcher and A. Nelson, *Tetrahedron: Asymmetry*, 2003, **14**, 1995–2004.
49 B. De Lange, W. F. Jager and B. L. Feringa, *Tetrahedron Lett.*, 1992, **33**, 2887–2890.
50 N. Berova, K. Nakanishi and R. W. Woody, in *Circular Dichroism: Principles and Applications*, Wiley-VCH, Weinheim, 2000.
51 L. Greb and J. M. Lehn, *J. Am. Chem. Soc.*, 2014, **136**, 13114–13117.
52 A. Hjelmencrantz, A. Friberg and U. Berg, *J. Chem. Soc., Perkin trans.*, 2000, **2**, 1293–1300.
53 H. S. Yu, X. He, S. L. Li and D. G. Truhlar, *Chem. Sci.*, 2016, **7**, 5032–5051.
54 J. Zheng, X. Xu and D. G. Truhlar, *Theor. Chem. Acc.*, 2011, **128**, 295–305.
55 A. V. Marenich, C. J. Cramer and D. G. Truhlar, *J. Phys. Chem. B*, 2009, **113**, 6378–6396.